Available online at www.sciencedirect.com
ScienceDirect
Journal of the European Ceramic Society 28 (2008) 1941–1951
www.elsevier.com/locate/jeurceramsoc

Assessment of viscoelastic crack bridging toughening in refractory materials

D.N. Boccaccini [a], M. Cannio [a,*], T.D. Volkov-Husoviæ [b], I. Dlouhy [c], M. Romagnoli [a], P. Veronesi [a], C. Leonelli [a]

[a] *Dipartimento di Ingegneria dei Materiali e dell'Ambiente, Università di Modena e Reggio Emilia, Via Vignolese 905, 41100 Modena, Italy*
[b] *University of Belgrade, Faculty of Technology and Metallurgy, Karnegijeva 4, POB 3503, Serbia*
[c] *Institute of Physics of Materials, ASCR, CZ-61662 Brno, Czech Republic*

Received 2 August 2007; received in revised form 21 December 2007; accepted 4 January 2008
Available online 5 March 2008

Abstract

Viscoelastic bridges can be formed in refractory ceramics while cooling from high temperatures. Such bridges can shield crack tips, thus reducing the effective crack tip stress intensity factors leading to higher resistance to creep and thermal shock. The extent to which the crack tip stress intensity is reduced can be estimated from fracture mechanics models that include experimental measurement of crack bridging and microstructural parameters. In this paper a novel approach is proposed for the assessment of the effective crack bridging toughening from combining destructive and non-destructive test methods. Fracture toughness values were determined applying chevron notched specimen technique and surface damage of the specimen was monitored by image analysis. Different cordierite–mullite compositions characterized by different microstructure morphologies and crack propagation behaviour were investigated. A brief discussion about the correlation between thermo-mechanical properties, microstructure, crack propagation behaviour and thermal shock resistance is presented. Moreover, an empirical model able to determine the presence and effectiveness of the viscoelastic crack bridging ligaments acting in the microstructure under thermal shock conditions and their degradation with increasing thermal shock cycles from parameters measured at room temperature is presented.

Keywords: Cordierite–mullite; Viscoelastic toughening; Fracture toughness; Image analysis; Fracture mechanics

1. Introduction

The characterization of thermal shock degradation of commercial refractories in service is of prime concern to the industry involving high temperature processes worldwide. When refractory materials are subjected to industrial thermal cycles crack nucleation and/or propagation occurs resulting in loss of stiffness, mechanical strength and overall material degradation. The subcritical damage processes promote a gradual chipping of the refractory material until the furnaces have to be shut down for the replacement of the brick or tiles. This results in significant economic losses, in term of lost production time and brick replacement costs. Despite the significance of the thermal shock problem, for example in the steel production processes, where the economical losses amount at least to millions of dollars,[1] the methods currently used in the prediction of thermal shock behaviour are based on the work of Hasselman[2] which was done more than 30 years ago. Since then, the subject of fracture mechanics has emerged as a powerful tool for the analysis of fracture problems and a number of researchers have applied fracture mechanics methods to the analysis of thermal shock.[1–6]

It has been demonstrated extensively in literature that viscoelastic toughening can improve the thermal shock behaviour of refractory materials.[1] Viscoelastic bridges, whose formation depends mainly on the viscosity–temperature characteristics of the glassy phase, have the net effect of shielding the crack tips from transient thermal stresses due to thermal shock.[1] Viscoelastic toughening has been observed in cordierite–mullite ceramics and explained elsewhere.[7,8] Briefly, the formation of viscoelastic ligaments was promoted by tailoring the magnesia, molochite, fused silica and alkali content in the refractory batch to raise the occurrence of a higher amount of glassy phase.[8] This

* Corresponding author. Tel.: +39 0592056284; fax: +39 0592056243.
E-mail address: cannio.maria@unimore.it (M. Cannio).

0955-2219/$ – see front matter © 2008 Elsevier Ltd. All rights reserved.
doi:10.1016/j.jeurceramsoc.2008.01.021

toughening mechanism is thought to be responsible for crack bridging, improving the resistance to creep and thermal shock in cordierite–mullite refractory ceramics. Likewise, crack blunting and/or crack bridging can play a more dominant role in the improvement of fracture toughness than the probable decrease of K_{IC} caused by the diminution of crack deflection due to the higher amount of glassy phase.

Unlike the case of grain bridging models in ceramics under mechanical loading, for which bridging models are well established, the only currently existing framework for the modelling of crack bridging under thermal shock conditions was developed by Bahr et al.[5] Most recently, the mechanics of the viscous-film bridging process has been modelled by McNaney et al.[9] using a self-consistent numerical model that incorporates microstructural parameters, such as grain size and the thickness of the grain-boundary film. The results of these analyses show that the shielding contributions from grain bridging increase with viscosity, grain aspect ratio, and test frequency, when all the other parameters are fixed. The relatively high complexity of these models has led to consider new methods to quantify the toughening efficiency of the observed phenomena of grain bridging in refractory materials.[7]

The aim of this work is to study the thermal degradation of different cordierite–mullite refractory compositions subjected to industrial thermal cycles by comparing the degradation curves obtained from image analysis with those obtained by fracture toughness determination applying chevron notched technique. The investigated materials are refractory plates used as support for the firing of porcelain articles in fast firing cycle kilns. An empirical mathematical model is proposed to determine quantitatively the efficiency of viscoelastic toughening present in cordierite–mullite refractory ceramics from the variation of fracture toughness values with thermal shock cycles coupled with specimen surface damage assessment from image analysis. This innovative empirical model, which uses a fracture mechanics approach, could permit significant resources and time savings in the design of the "best" refractory plates for a given application.

2. Experimental

2.1. Materials and processing

Three different series of refractory plates of cordierite–mullite composition, indicated as RSE, AR004 and BRT, were prepared with the aim to provide refractory plates to be used as supports in whiteware fast firing cycles. These cordierite–mullite refractory materials were sintered for 2 h at 1250 °C. The complete description of the manufacturing details of these refractory plates is described elsewhere.[7] Table 1 provides the chemical composition of fired bodies and Table 2 summarizes the main thermo-mechanical properties of the refractory materials investigated. From a compositional point of view, RSE material has the lowest content of glassy phase due to its lower amount of silica and alkalis, while AR004 material presents higher amount of SiO_2 and alkali content while lower Al_2O_3 content, as evidenced in Table 1. The chemical composition plays a major role in the characteristics of the aggregate–matrix bond interface, which determines the main thermo-mechanical properties of refractory materials, i.e. thermal shock resistance. It can be considered that BRT material has an intermediate amount of glassy phase in comparison with the other compositions. Moreover, BRT contains higher amount of Mg than RSE material but similar Mg content than AR004. Table 2 evidences that AR004 material is the densest material and it presents the highest fracture strength and fracture toughness values at room temperature. However, these high mechanical properties at room temperature do not signify necessary good thermo-mechanical properties, i.e. thermal shock resistance, as discussed above.

Table 1
Chemical composition of the two refractory samples investigated (RSE and BRT) (in wt%)

Oxide	wt%		
	RSE	BRT	AR004
SiO_2	43.14	46.42	48.56
Al_2O_3	45.51	41.51	39.67
CaO	0.59	0.74	0.76
MgO	8.09	8.32	8.30
Na_2O	0.05	0.12	0.17
K_2O	0.51	0.64	0.74
Fe_2O_3	1.55	1.52	1.49
TiO_2	0.57	0.71	0.31
Total	100.00	100.00	100.00

2.2. Microstructural characterization

Representative samples from each of the material were subjected to standard ceramography techniques. Scanning electron microscopy (SEM) (PHILIPS XL 40) was performed to characterize the microstructure of the refractory materials, coupled with energy dispersive spectroscopy (EDS). The EDS technique was particularly important for obtaining semi-quantitative information on the composition of the grain–matrix interface.

Table 2
Physical, thermal and mechanical properties of the as-received RSE, AR004 and BRT refractory materials

Parameter	RSE	BRT	AR004
Bulk density, ρ (g/cm^3) (*)	2.08	1.91	2.2
Thermal expansion coefficient, α (25–1250 °C) ($\times 10^{-6}$ °C^{-1})	3.06	2.49	3.09
Apparent porosity (%)	24	28	22
Dynamic Young's modulus, E_{dyn}, impulse excitation technique (I.E.T.) (GPa)	21.5	15.7	23.7
Dynamic Poisson's ratio, μ_{dyn}, impulse excitation technique (I.E.T.)	0.16	0.16	0.16
Three-point bending strength, σ (MPa)	22	26	30
Fracture toughness, K_{IC} (MPam$^{1/2}$)	0.36	0.52	0.56

* GeoPyc 1360 Micromeritics, Norcross, GA 30093-1877, U.S.A (reproducibility ±1.1%).

2.3. Thermal shock experiments

The performance of the refractory plates was tested on-duty in industrial whiteware kilns following the thermal treatment employed in fast firing cycles (maximum temperature between 1250 and 1275 °C). Hence, the number of thermal shock experiments hereafter considered corresponds to the number of fast firing cycles carried out on the refractory plates. The term "thermal shock" is used throughout the text in agreement with the literature on refractory materials. 50 refractory plates of each composition were marked and followed during all their service life. 34 plates of BRT material survived 510 cycles without visible fractures, while for RSE material the number of plates was only 16. In the case of AR004 material, the complete sample lot was broken at 510 cycles. In many refractory plates, even if cracks were already visible after few thermal cycles, the propagation through the transversal direction of the plates occurs in relatively slow mode.

The refractory materials exhibit different thermal shock failure mechanisms, i.e. RSE being characterized by early crack initiation and slow crack propagation, while BRT exhibiting delayed crack initiation and fast fracture propagation.[7,10] The best performance under service life relevant thermal shock conditions was achieved with BRT refractory material composition, while AR004 showed a catastrophic crack propagation behaviour under the same conditions.

2.4. Three-point bending strength

Fracture strength data were determined at room temperature before and after 110, 360 and 510 industrial thermal cycles. The prismatic bars of dimensions 80 mm × 25 mm × 5 mm used for these measurements were cut from the refractory plates using a diamond saw. Tests were carried out in three-point bending configuration with a 70 mm span and a cross-head speed of 3 mm/min using a universal testing machine (MTS 810, USA). At least 10 samples for each condition were tested and the results were averaged. The fracture strength was calculated by using the following equation:

$$\sigma_f = \frac{3PL}{2BW^2} \tag{1}$$

where P is the maximum load, L the span, B the width of the specimens and W their thickness.

2.5. Dynamic Young's modulus determination from ultrasonic pulse velocity testing

A commercial ultrasonic testing instrument of transmission type (PUNDIT *plus* PC1006, CNS Farnell Ltd., Hertfordshire, England) was used. The instrument consists of a pulse generator and timing circuit coupled to two transducers (220 kHz) that were positioned manually at opposite ends of each specimen. Each transducer had a 2-mm thick rubber tip to help overcome measurement problems due to the roughness of the refractory surface. The ultrasonic velocity, v, is calculated from the distance between the two transducers and the electronically measured transit time of the pulse as:

$$v\,(\mathrm{m/s}) = \frac{\mathrm{d}}{t} \tag{2}$$

where d = distance between the two transducers (m) and t = transit time (s).

By determining the ultrasonic velocity and bulk density (ASTM C-134) of a refractory it is possible to calculate the dynamic modulus of elasticity using the equation below (ASTM C 1419-99a):

$$E_{\mathrm{dyn}} = v^2\rho\left(\frac{(1+\mu_{\mathrm{dyn}})(1-2\mu_{\mathrm{dyn}})}{1-\mu_{\mathrm{dyn}}}\right) \tag{3}$$

where v is pulse velocity (m/s), ρ the density (kg/m^3) and μ_{dyn} the dynamic Poisson's ratio.

Each test of ultrasonic velocity measurement was run at least 5 times to correctly determine the ultrasonic velocity and the values reported are the mean value of the measurements performed on the refractory plates surviving 0, 110, 360 and 510 industrial thermal cycles. The complete description of the ultrasonic pulse velocity testing method and its application to characterize thermal shock damage degradation in refractory materials has been presented in preliminary studies.[11,12]

2.6. Fracture toughness determination

Fracture toughness data of selected samples before and after industrial thermal cycles were obtained by the chevron notch (CN) technique at room temperature. The specimen geometry employed in this test was a bar with dimensions W = 4 mm, B = 3 mm, l = 16 mm, where W = thickness, B = width and l = rollers span, respectively. Chevron notches with angles of 90° were cut using a thin diamond wheel. The specimens were loaded in three-point bending configuration at a constant cross-head speed of 0.01 mm/min. Graphs of load versus deflection were recorded and the fracture toughness was calculated from the maximum load (F_{max}) and the corresponding minimum value of geometrical compliance function (Y^*_{min}) using the following equation[13]:

$$K_{\mathrm{Ic}} = \frac{F_{\mathrm{max}}}{BW^{1/2}}Y^*_{\mathrm{min}} \tag{4}$$

where B and W are the width and thickness of the specimens, respectively. The calculation of the function Y^*_{min} for chevron notched bending bars was based on Bluhm's slice model.[14] The calculation procedure used for the purposes of this investigation has been described in detail elsewhere.[13] The chevron notch depth (a_0) was measured from optical micrographs of broken specimens.

The measurement of fracture toughness was performed in as-received plates and after 110, 360, 510 thermal shock cycles.

2.7. Image analysis

Photographs of thermally degraded specimens were taken before and after 110, 360 and 510 industrial thermal shock cycles. IMAGE PRO PLUS software (Materials_Pro® Analyzer,

Version 3.1, Media Cybernetics, Silver Spring, MD, USA) was used for image analysis. The specimens were covered with thin chalk-powder film before surface damage was investigated. Chalk powder is employed to colour the refractory surfaces to differentiate between damaged and non-damaged areas. The chalk powder used was selected between the commercially available products taking into account the powders showing the higher contrast, the lack of reactivity with the refractory specimen investigated and the price. When it is chosen the appropriate colour, it is possible to quantitatively measure the ratio and level of damaged and non-damaged areas by means of image analysis using a statistical approach. The area without damage is

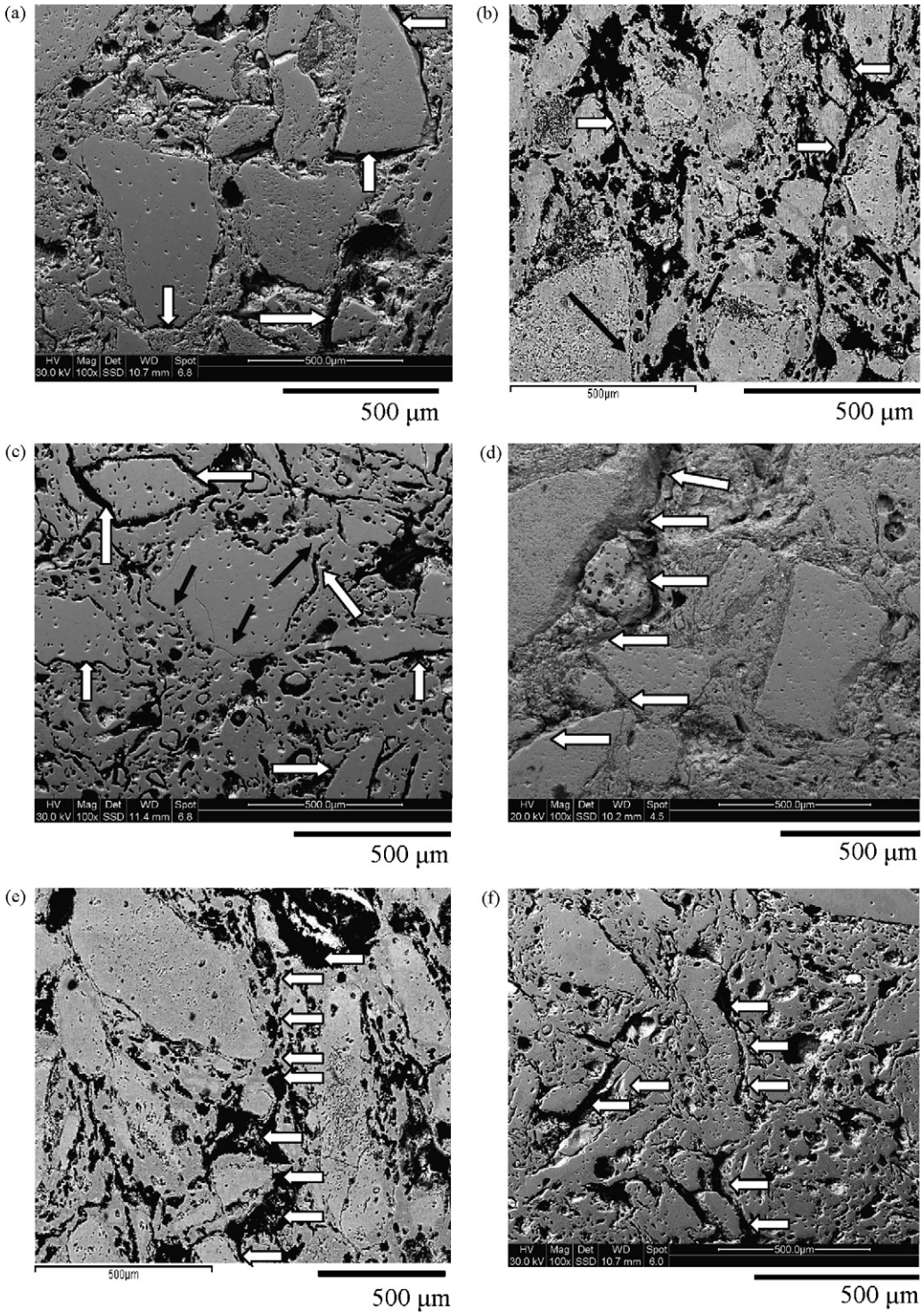

Fig. 1. SEM micrographs of polished sections of refractory samples at low magnification for: (a) RSE, (b) AR004, (c) BRT samples, showing different microstructural features before thermal cycling exposition; while (d)–(f) corresponds to samples of RSE, AR004 and BRT refractory materials after 110 thermal shock cycles (white arrows indicate microcracking while black arrows crack bridges).

in general coloured by the chalk powder in the majority of the experiments, while the damaged areas keep the basic colour of the refractory materials. This method of colouring the refractory samples depends on the bonding present between the chalk powder and the original surface of the refractories. Good quality bonding can be defined when chalk powder is on the non-damaged surface, and it could not be removed unless brush or sponge is used. If this bonding is strong enough, then chalk powder is likely on the non-damaged area of the sample. However, if the bonding is weak and the value of the damage area is close to that of the grain diameter, the chalk powder should colour the damaged area. The film provided better contrast and differentiation of damaged and non-damaged surfaces.[15]

The ratio between sample surface area (P_0) and damaged surface area (P) was calculated for each refractory material and stage of thermal cycling. The results of $((P_0/P)\%)$ ratio against number of thermal shock cycles for all the compositions were plotted. At least 10 photographs/sample were analysed to obtain a reliable characterization of the microstructure. Refractory specimen surfaces were fresh, as any additional process could damage the original state of the sample.

3. Results

3.1. Microstructural observations

Fig. 1 shows the microstructures observed before thermal cycling exposition of cordierite–mullite refractory materials; a, b and c correspond to RSE, AR004 and BRT samples, respectively. Fig. 1d–f report microstructure of these refractories after 110 thermal shock cycles. At first glance the microstructures of the refractory samples appear very different, with RSE samples exhibiting a less dense and interconnected microstructure than BRT and AR004 samples, as observed in the SEM images in Fig. 1a–c, respectively. RSE samples show a microstructure with large and well defined grains not connected by any amorphous continuous phase (Fig. 1a). In the RSE material the interconnected porosity amounts 24%, as evaluated by 2D image analysis, while for the BRT sample the porosity is 28% (Table 2). In both materials pores are not spherical, indicating an early stage of sintering.[16] A detailed examination of SEM micrographs of Fig. 1a–c (no thermally cycled samples) indicates that the materials were extensively microcracked and cracks were predominantly intergranular (see white arrows in Fig. 1a–c). Although both materials present random orientation of these pre-existing cracks, the BRT material shows smaller pore sizes for both matrix and grain microstructure. The crack amount and morphology can be quantitatively characterized by the statistical determination of the roundness parameter by means of image analysis.[17] SEM micrographs of the microstructure of samples after 110 cycles show that for both materials the major cracking event might be better described as aggregate–matrix bond interface separation, as can be seen in Fig. 1d–f; the white arrows indicate possible paths of crack propagation. In the cordierite–mullite composites examined in this work, it is thought that the interaction between aggregate–matrix bond interface cracks and matrix flaws is the effect playing a major role on the mechanical properties. The mean distance between aggregate and matrix bond interface cracks was determined by image analysis measurement on a representative number of microstructure micrographs. The measured mean values of the distance between cracks are of the order of the crack length and approximately equivalent to the aggregate grain dimension, being 600 μm for RSE and 450 μm for BRT materials, respectively in the as-received state. Indeed, as Fig. 1(a and d) shows, the larger aggregate grains of RSE material appear to have a significant function of providing the connectivity between cracks after thermal shock experience. Moreover a higher amount of porosity and interconnected cracks was observed in the case of AR004 material.

Fig. 2a reports a SEM micrograph of a bridging ligament, indicated by the dark arrow, present in the microstructure of a BRT sample, while Fig. 3a–c report EDS spectra corresponding to the areas labelled (1), (2) and (3) in Fig. 2a, respectively. The EDS spectra of Fig. 3 report the chemical composition of the refractory matrix (area 1), of an extensive area of the aggregate microstructure (area 2) and a point into the aggregate silicate matrix (area 3), respectively. In particular, the EDS spectrum of Fig. 3c corresponding to the aggregate silicate matrix composition, put in evidence the presence of Mg inside the molochite

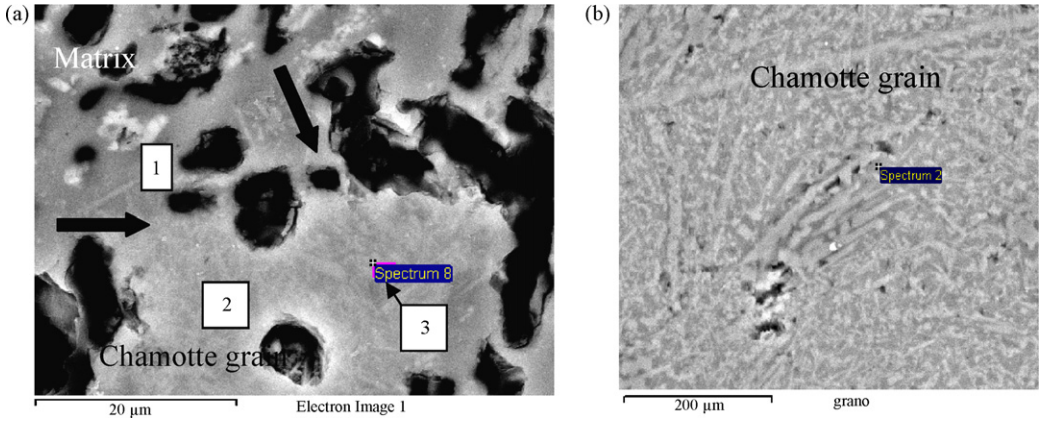

Fig. 2. (a) SEM micrograph of a bridging ligament present in the microstructure of a BRT sample (b) SEM micrograph of the molochitic grain matrix of a BRT sample (black arrows indicate crack bridges).

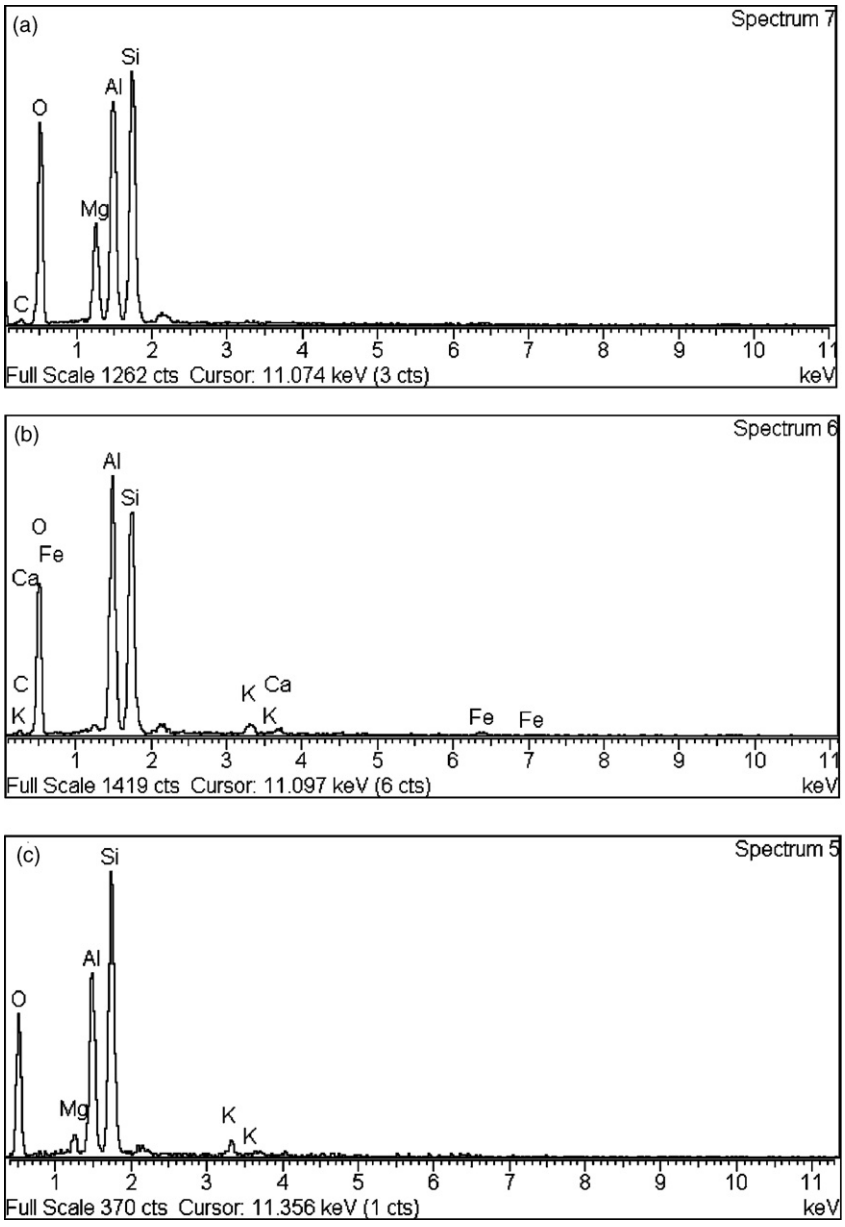

Fig. 3. EDS spectra of the areas labelled (1), (2) and (3) in Fig. 2(a) for BRT material, corresponding to the chemical composition of the refractory matrix, of an extensive area of the aggregate microstructure and a point into the aggregate silicate matrix, respectively.

grain, which could indicate the diffusion of Mg inside the molochite grains from the cordieritic matrix. This latter assessment delays in the fact that no traces of Mg was found in both ICP and EDS analyses performed on the molochite grog used as raw material.[8] A SEM micrograph of the microstructure of a molochitic grain can be observed in Fig. 2b. A complete description of the formation of toughening mechanisms (i.e. viscoelastic toughening) in cordierite–mullite refractories as function of the raw materials employed (chemical composition, chamotte amount, etc.) is described elsewhere,[7] and it is the focus of a manuscript in preparation.[8] The aggregate–matrix bond interface is deeply related with thermal shock behaviour in refractory materials.[1] It is wished that crack arising from thermal stresses after thermal shock experience in these interface has to be stopped. Ion diffusion mechanisms and chemical reactions able to develop weak interphases in these aggregate–matrix interfaces during manufacturing firing (and to re-create or restore again on-duty the high temperature cycles) could certainly improve the lifetime of the refractory specimens. It has been observed,[8] that the use of fused silica in the grog batch can promote the development of multilayer glassy phases surrounding these fused silica grains. The evolution of these glassy phases with temperature indicates that after approximately 100 °C the glass become viscous and a crack blunting toughening mechanism could be expected. On cooling after a thermal shock experience, this glass could induce crack branching and crack shielding effects on the propagating cracks improving the overall fracture toughness property of the material. Moreover, at high temperatures, Mg ions can diffuse from the cordieritic matrix into the glassy phase of the molochite grains, decreasing the thermal expan-

sion coefficient mismatch between these two phases, enabling the formation of crack bridging on cooling. This mechanism of diffusion is promoted by the amount and by the viscosity of these glassy phases (the cordieritic matrix of the material and the aluminium silicate matrix of the aggregates); which, in turn, depends strongly on the overall silica and alkali content of the raw materials employed. However, there is a compromise between the amount of glassy phase to promote viscoelastic crack bridging by Mg ion diffusion and thermal shock resistance of the material, since glassy phase in excess could induce transgranular crack propagation leading to higher crack growth rates. This later behaviour could be the reason of the poor thermal shock behaviour observed in AR004 material, despite it shows the highest values of fracture toughness and fracture strength in the as-received condition.

3.2. Fracture strength–ultrasonic velocity correlation

Refractory materials inevitably contain some flaws in the form of porosity, microcracks and impurities. When ceramics containing inherent flaws are subjected to severe thermal shock, damage concentrated at tips of those pre-existing flaws will be generated leading to higher number of microcracks and hence the fracture strength will be degraded. The change in strength as a function of the cumulative number of thermal shock cycles is presumably due to the accumulation and coalescence of thermal shock-induced microcrack damage.[18]

Fig. 4 shows the effects of the industrial thermal shock cycles on fracture strength and ultrasonic velocity, measured through the length (v_L), of the refractory plates. The values are given relative to the mean values of fracture strength and ultrasonic velocity measured on as-received samples of BRT material. It is evident observing Fig. 4 that the fracture strength of RSE material is higher than that of BRT in the as-received condition. The strength of both materials decreases initially rapidly, in particular for RSE material, and after about 100 thermal shock cycles the values tend to saturation with increasing number of cycles.

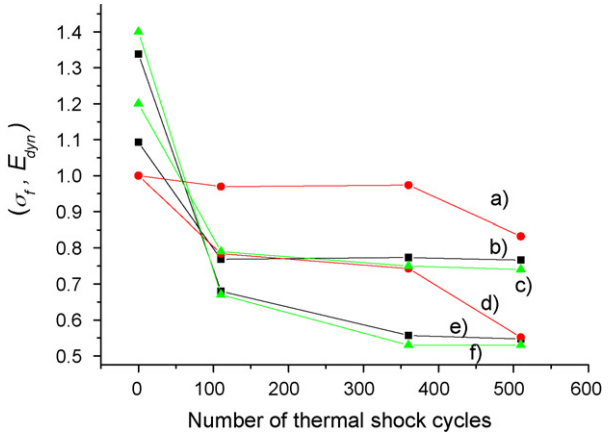

Fig. 4. Fracture strength and dynamic Young's modulus as function of number of thermal shock cycles, where the curves labelled (a) corresponds to σ_f of BRT, (b) E_{dyn} of RSE samples, (c) E_{dyn} of AR004, (d) E_{dyn} of BRT and (e) σ_f of RSE and (f) σ_f of AR004 material, respectively. The values are given relative to the values of fracture strength and dynamic Young's modulus measured on samples before thermal shock. The average relative standard deviation is less than 5%.

Fig. 4 also shows a remarkable similarity between the trends of σ_f and v, as can be observed comparing the curves labelled (a)–(d), (b)–(e) and (c)–(f), where curves (a)–(c) correspond to σ and v of BRT material (b)–(d) to RSE material and (c)–(f) to Ar004, respectively. This fact can be explained considering the Griffith theory.[19] In a previous investigation it was demonstrated that the on-duty fracture of these refractory plates can be correlated to a single dominant phenomena with a major crack aligned in parallel to the transversal direction of the sample.[11] The suitable set-up of the UPV transducers during the measurement of v_L permitted the detection of the onset of crack initiation and the progress of further microcracking development into macroscopic damage. The critical length sizes were found to be ~700 and ~500 μm for BRT and RSE refractory plates, respectively (results not shown here). Longer cracks will propagate at higher crack-growth rates, as demonstrated in Ref. [12] In many of the investigated samples, cracks are already visible after approximately 100 cycles, with crack lengths higher than 1 mm.[11]

The retained strength after 110 cycles is approximately 90% for BRT material while RSE material retains only 70%. When

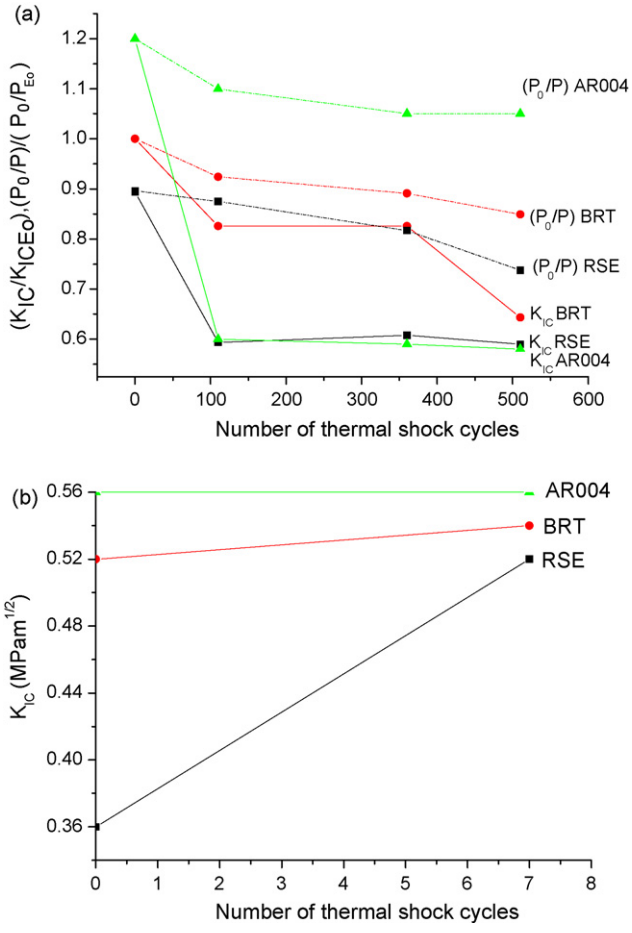

Fig. 5. (a) K_{IC} and surface damage values (P_0/P) against number of thermal shock cycles. (b) K_{IC} values in the 0–7 thermal shock range determined by the chevron notched technique.

the number of cycles is 360, the retained strength of the refractory materials remains almost constant, about 90% for BRT and 70% for RSE, respectively. The higher retained strength of BRT material indicates that it should behave better under thermal shock conditions. In fact from the 50 refractory plates studied of each composition, 34 plates of BRT material survived 510 cycles without visible fractures, while for RSE material the number of undamaged plates was only 16. Such damage of RSE material could be induced by stresses arising from thermal expansion mismatch between the coarse grain aggregates (molochite, fused silica, etc.) and the cordieritic matrix (see microstructure image, Fig. 1a). Thermal expansion anisotropy of the aggregate grains and stresses from the non-linear temperature distribution present during the thermal cycles, as explained in previous investigations,[7,10] should also contribute to the observed different behaviour of the materials.

3.3. Fracture toughness–surface damage parameter correlation

Fig. 5a shows the variation of K_{IC} and surface damage parameter ($(P_0/P)\%$) with number of industrial thermal shock cycles. The values are given relative to the fracture toughness and damage surface of as-received BRT samples. It is evident that AR004 presents higher values of K_{IC} than BRT and RSE material during all their service life, but a more severe decrease with thermal shock cycles. Likewise there is a clear significant correspondence between the trends of K_{IC} and P_0/P for all the investigated materials. This could be due to the capability of image analysis to monitor the development of surface degradation, which is strongly related to the quality of the interface between mullitic aggregate grains and cordieritic matrix. Thermal shock cycles induce thermal damage in the microstructure, leading to weakening of this interface and as consequence the grains can be removed easier, i.e. optical microscopy images of Fig. 6(a and b) confirm the presence of grain pull-out effect in the as-received conditions for all the compositions investigated, but in particular with higher frequency in RSE composites. Optical micrographs of fracture surfaces obtained on thermally shocked samples (110 cycles) after fracture toughness test (not reported here) confirmed the presence of grain pull-out effects in both compositions, but in particular with higher frequency in RSE composites. The more detailed analysis of fracture morphology has been presented elsewhere.[20,21] When the specimens were covered with thin chalk-powder film, the grain pull-out effect was evident from the optical microscopy images used for P_0/P ratio assessment, reported in Fig. 6(a and b). The higher fracture toughness values of AR004 and BRT materials (Fig. 5a) can be mainly attributed to the presence of silicate glassy phases in the mullitic-aggregates/cordieritic–matrix interface and to the higher amount of cordieritic matrix, in comparison to RSE material. The effect of microstructure on fracture toughness has been investigated elsewhere.[7] The presence of this glassy cordieritic matrix is thought to be responsible for crack tip blunting, shielding and crack bridging, while the silicate glassy phases in the grain–matrix interface can lead to crack branching toughening mechanisms as explained before. It is thought that these toughening mechanisms can play a more dominant role in the improvement of fracture toughness than the probably decrease of K_{IC} caused by the diminution of crack deflection due to the higher amount of glassy phase. In addition, the smaller size of mullitic aggregates of BRT material leads to better

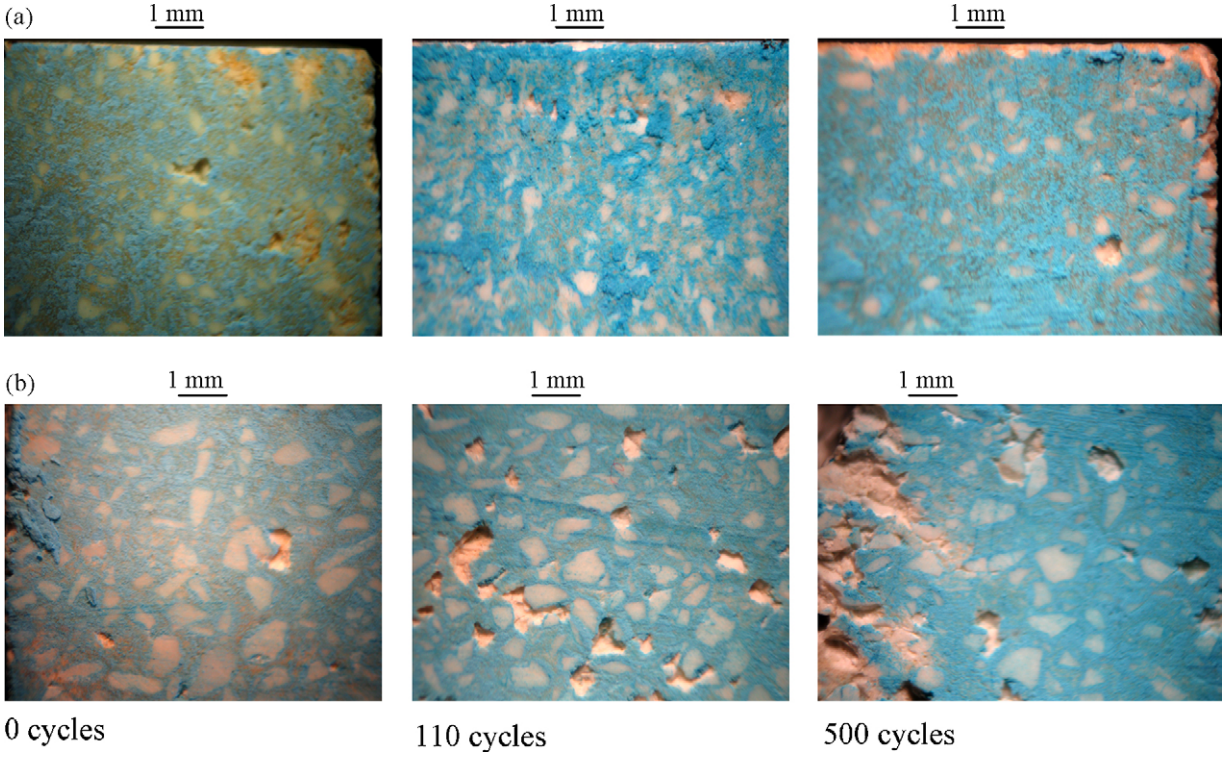

Fig. 6. Images of surface degradation for samples before and after 110 and 510 thermal shock cycles for (a) BRT and (b) RSE refractory materials.

thermo-mechanical properties including lower thermal expansion coefficient.[8]

An unexpected increasing trend of K_{IC} values for both refractory compositions was found in the first seven cycles, in particular for RSE material, as Fig. 5b depicts. After 15 industrial thermal cycles, the fracture toughness trend of BRT material is less pronounced than for RSE, suggesting again that BRT is less sensitive to repeated thermal shocks than RSE material. From an industrial point of view, where a reliable parameter is desired which can be used to extrapolate the behaviour of the material after few cycles, it seems that the σ_f/σ_0 ratio is more suitable than K_{IC}/K_{IC0} ratio, since the former does not present the initial increasing trend, hence after fewer number of initial cycles the thermal shock behaviour can be predicted. Increase in fracture toughness after seven thermal shock cycles could be assigned to a crack shielding effect at grain boundaries.[20] This effect should be high in the coarse grained material (RSE) (Fig. 1a) whereas for the fine grained materials, BTR and AR004, Fig. 1b and c respectively; the effect should be negligible.

Fig. 7(a and b) shows the trends of fracture toughness (K_{IC}) against surface damage parameter (P_0/P) plotted in logarithmic scale for all the compositions investigated. Fitting the experimental data of $\ln K_{IC}$ against $\ln((P_0/P)\%)$ with a linear trend it is possible to express the correlation fracture toughness–surface damage parameter with the following equation:

$$K_{IC} = K_{IC0}\left(\frac{P_0}{P}\right)^b \quad (5)$$

where K_{IC0} is the fracture toughness of the materials in the as-received state, P_0 = sample surface before thermal degradation, P = damage surface and b = material constant (2.45 in the case of BRT material).

The variation of the surface damage parameter ($(P_0/P)\%$) can be mainly attributed to grain pull-out due to embrittlement of the viscoelastic ligaments between grain–matrix interface with thermal shock cycles. In the case of AR004 and BRT material, the high correlation coefficient between K_{IC} and P_0/P could indicate an efficient viscoelastic toughening by crack bridging and as consequence the grain-pull increase due to thermal degradation could be related to the decreasing amount of viscoelastic ligaments. On the other hand, RSE is the refractory composition showing lower fracture toughness. In this case, it can be assumed that viscoelastic bridging is negligible and this assessment is in agreement with the images observed in Fig. 6. The presence of grain-pull effect in RSE material is evident from optical microscope observation even before submitting the specimens to thermal shock, and hence it is not possible to find correlation between fracture toughness variation and surface damage parameter with number of thermal shock cycles. Therefore, the correlation coefficient between K_{IC} and P_0/P, varying between 0 (bad) and 1 (excellent), could be used as a qualitative–quantitative technological parameter to characterize the presence and influence of viscoelastic crack bridging in fracture toughness, creep and hence thermal shock resistance by combining destructive and non-destructive techniques.

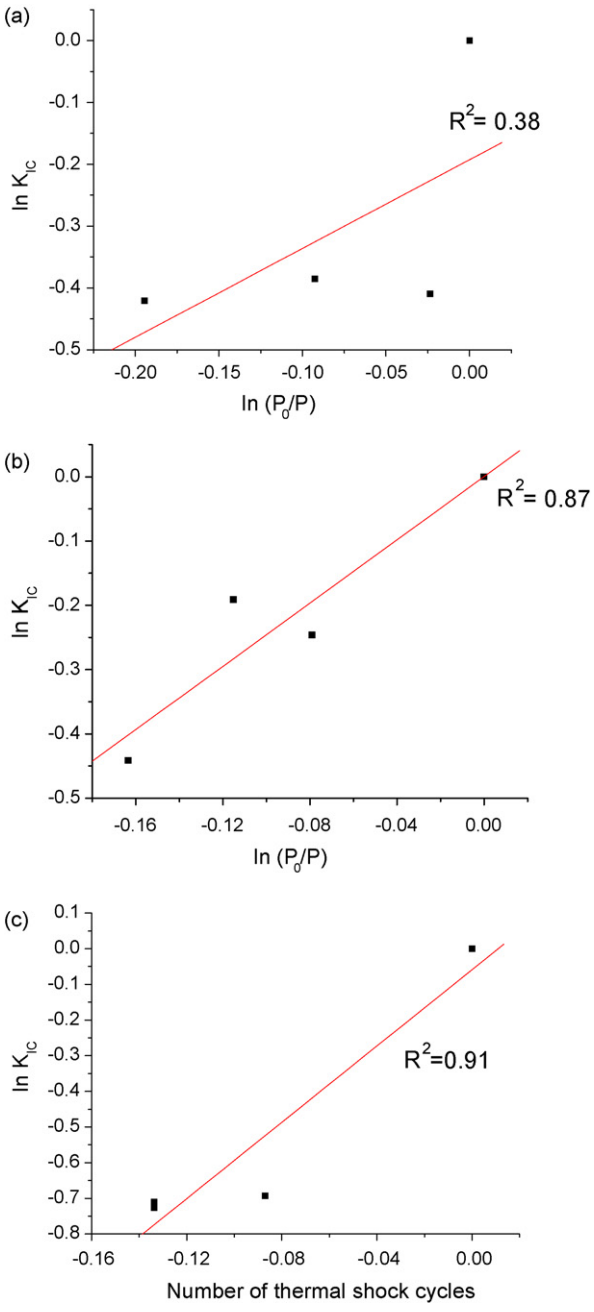

Fig. 7. (a) Fracture toughness (K_{IC}) against surface damage parameter (P_0/P) plotted in logarithmic scale for (a) RSE and (b) BTR samples (c) AR004 samples.

Fig. 8 plots the variation of ratio of fracture strength difference and dynamic Young's modulus difference $d\sigma_f/dE_{dyn}$ with thermal shock cycles for the materials investigated. This parameter has been suggested in our previous investigation[22] to characterize the thermal shock behaviour in refractory materials. This parameter has very high sensibility to detect change in the materials properties due to thermal degradation and hence it can be used to distinguish quantitatively the thermal shock behaviour of refractories.

It is noticeable the different trends of $d\sigma_f/dE_{dyn}$ for the materials here investigated. AR004, the refractory material having a catastrophic failure due to the strong interface between the

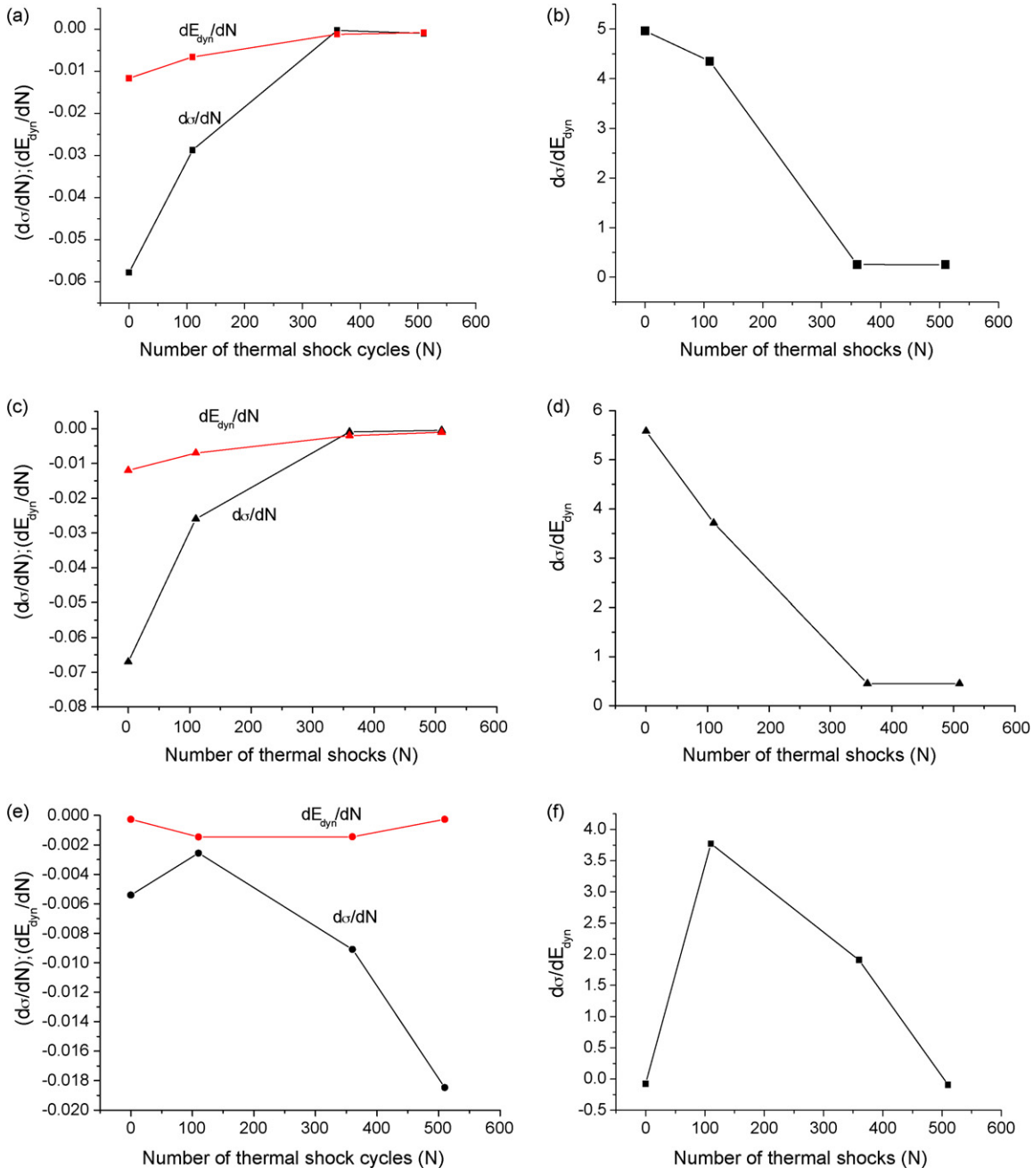

Fig. 8. dE_{dyn}/dN, $d\sigma/dN$ and $d\sigma/dE_{dyn}$ ratio with number of thermal shock cycles for RSE (a and b), AR004 (c and d) BTR (e and f) RSE samples.

cordierite matrix and mullite grains, shows the most severe decreasing trend of $d\sigma_f/dE_{dyn}$ ratio with thermal shock cycles (Fig. 8d). RSE material (Fig. 8b) has the lowest values of fracture toughness in the as-received condition and lack of crack bridging, as mentioned above. The decreasing trend of $d\sigma_f/dE_{dyn}$ ratio during all their service life indicate a higher rate of degradation of fracture strength in comparison with dynamic Young's modulus. On the other hand, BRT material (Fig. 8f) has intermediate fracture toughness values and crack bridging toughening, but it shows an increasing almost linear trend of $d\sigma_f/dE_{dyn}$ values in the first ~100 thermal shock cycles. This is due to the lower degradation rate of fracture strength in comparison with the Young's modulus, for increasing thermal shock cycles. However, after ~100 thermal shock cycles, the $d\sigma_f/dE_{dyn}$ trend changes decreasing linearly up to the end of the material's service life. Considering that the main toughening mechanism present in BRT material, and not found in the other refractory compositions, is viscoelastic crack bridging, the slight degradation of this mechanism with thermal shock could be represented by the almost linear initial increasing trend of $d\sigma_f/dE_{dyn}$. After approximately 100 thermal cycles, the thermal shock cycles have irremediably reduce the capability of formation of viscoelastic bridges of BRT material and then undergoes a decreasing almost linear trend up to the end of the material service life, with a degradation rate comparable with the other refractory materials.

4. Conclusion

In refractory materials, the resistance to thermal shock can be improved by means of microstructural viscoelastic bridging. For the design of high temperature ceramics it is very useful to obtain a reliable parameter from which it is possible to assess the presence of viscoelastic bridging in the material microstructure, given support to the other methods as SEM observation and/or theoretical viscoelastic models. In this investigation it is demonstrated the good agreement between the surface damage parameter variation (determined by the image analysis method here described) and the increase of grain pull-out effect in refractory materials with thermal shock cycles. The quantity of grain pull-out is deeply related to the overall fracture toughness property of refractory materials and the presence of effective crack bridges acting in the material microstructure should play a major role in the conservation of this property despite of the thermal shock degradation occurring throughout all the service life. Hence, in this work it is proposed the correlation coefficient between experimental (measured) fracture toughness values and damage surface parameter monitored by image analysis against number of thermal shock cycles as a novel empirical technological parameter able to detect the presence and influence of viscoelastic bridging in the material performance. In addition, the variation of ratio of fracture strength difference to Young's modulus $d\sigma_f/dE_{dyn}$, with number of thermal shock cycles can be used to study the degradation of these viscoelastic ligaments under thermal and/or mechanical loading conditions. These combination between destructive (K_{IC}) and non-destructive ($(P_0/P)\%$) characterization techniques gives a complete description of the refractory material performance under thermal loading and permit to predict their future behaviour when subjected to real on-duty conditions. Moreover it represents a complementary characterization tool for the design of refractory materials under a fracture mechanics approach.

Acknowledgments

D. Boccaccini wish to thank all the technicians at the University of Modena and Reggio Emilia, who help me throughout my PhD Thesis, as some results are presented in this work. Part of the research was financially supported by Czech Science Foundation (Project No. 106/05/0495).

References

1. Soboyejo, W. O. and Mercer, C., Investigation of thermal shock in a high-temperature refractory ceramic: a fracture mechanics approach. *J. Am. Ceram. Soc.*, 2001, **84**(6), 1309–1314.
2. Hasselman, D. P. H., Unified theory of thermal shock fracture initiation and crack propagation in brittle ceramics. *J. Am. Ceram. Soc.*, 1969, **52**(11), 600–604.
3. Swain, M. V., Lutz, E. H. and Claussen, N., K_R-curve behavior of duplex ceramics. *J. Am. Ceram. Soc.*, 1991, **74**, 11–18.
4. Bahr, H. A., Weiss, H. J., Maschke, H. G. and Meissner, F., Multiple crack propagation in strip caused by thermal shock. *Theor. Appl. Fract. Mech.*, 1988, **10**, 219–226.
5. Bahr, H. A., Fett, T., Hahn, I., Munz, D. and Pflugbeil, I., Fracture mechanics treatment of thermal shock and the effect of bridging stresses. In *Thermal Shock and Thermal Fatigue Behaviour of Advanced Ceramics*, ed. G. A. Schneider and G. Petzow. Kluwer, Dordrecht, The Netherlands, 1993.
6. Ramamurty, U., Retardation of fatigue crack growth in ceramics by glassy ligaments: a rationalization. *J. Am. Ceram. Soc.*, 1996, **79**, 945–952.
7. Boccaccini, D. N., Leonelli, C., Rivasi, M. R., Romagnoli, M. and Boccaccini, A. R., Microstructural investigations in cordierite–mullite refractories. *Ceram. Int.*, 2005, **31**(3), 417–432.
8. Boccaccini, D. N., Viscoelastic crack bridging promoted by fused silica chamotte and Mg ion diffusion in cordierite–mullite ceramics; manuscript in preparation.
9. McNaney, J. M., Gilbert, C. J. and Ritchie, R. O., Effect of viscous grain bridging on cyclic-fatigue-crack growth in monolithic ceramics at elevated temperatures. *Acta Metall. Mater.*, 1999, **47**, 2809–2819.
10. Boccaccini, D. N., Leonelli, C., Romagnoli, M., Pellacani, G. C., Veronesi, P., Dlouhy, I. *et al.*, Thermal shock behaviour of mullite–cordierite refractory materials. *Adv. Appl. Ceram.*, 2007, **106**(3), 142–148.
11. Boccaccini, D. N., Romagnoli, M., Kamseu, E., Veronesi, P., Leonelli, C. and Pellacani, G. C., Determination of thermal shock resistance in refractory materials by ultrasonic pulse velocity measurement. *J. Eur. Ceram. Soc.*, 2007, **27**(2–3), 1859–1863.
12. Boccaccini, D. N., Romagnoli, M., Veronesi, P., Cannio, M., Leonelli, C., Pellacani, G. C. *et al.*, Quality control and thermal shock damage characterization of high-temperature ceramics by ultrasonic pulse velocity testing. *Int. J. Appl. Ceram. Technol.*, 2007, **4**(3), 260–268.
13. Boccaccini, A. R., Rawlings, R. D. and Dlouhy, I., Reliability of chevron-notch technique for fracture toughness determination in glass. *Mater. Sci. Eng. A*, 2003, **347**, 102–108.
14. Bluhm, J. I., Slice synthesis of a three dimensional work of fracture specimen. *Eng. Fract. Mech.*, 1975, **7**, 593–604.
15. Volkov-Husoviæ, T. D., Janèiæ, R. M. and Mitrakoviæ, D., Image analysis used to predict thermal stability of refractories. *Am. Ceram. Soc. Bull.*, 2005, **84**(10), 1–5.
16. German, R. M., Fundamentals of sintering. *Ceramics and Glasses: Engineered Materials Handbook*, *vol. 4*. ASM International, USA, 1991, p. 262.
17. Baxes, G. A., *Digital Image Processing Principle and Applications*. John Wiley and Sons Inc., New York, USA, 1994, p. 157.
18. Boccaccini, A. R., Ponton, C. B. and Chawla, K. K., Development and healing of matrix microcracks in fibre reinforced glass matrix composites: assessment by internal friction. *Mater. Sci. Eng. A*, 1998, **241**, 141–150.
19. Gdoutos, E. E., *Fracture Mechanics: An Introduction*. Kluwer Academic Publishers, Dordrecht, Boston, London, 1993.
20. Chlup, Z., Dlouhy, I., Boccaccini, A. R., Boccaccini, D. N., Leonelli, C. and Romagnoli, M., Thermal shock resistance of cordierite–mullite refractory composites. *Key Eng. Mater.*, 2005, **290**, 260–263.
21. Chlup, Z., Boccaccini, D., Leonelli, C., Romagnoli, M. and Boccaccini, A. R., *Silikáty*, 2006, **50**, 245.
22. Boccaccini, D. N., Kamseu, E., Volkov-Husoviæ, T. D., Cannio, M., Romagnoli, M., and Veronesi, P., *et al.*, Service life prediction models for refractory materials. *J. Mater. Sci.*; in press.